2017

Picosecond Yb-Doped Fiber Amplifier

Weibin Zhu
University of Central Florida

PICOSECOND YB-DOPED FIBER AMPLIFIER

by

WEIBIN ZHU
B.S. South China Normal University, 2015

A thesis submitted in partial fulfillment of the requirements
for the degree of Master of Science
in CREOL – College of Optics & Photonics
at the University of Central Florida
Orlando, Florida

Spring Term
2017

Major Professor: Rodrigo Amezcua Correa

ABSTRACT

Due to its versatility, rare earth doped fiber amplifier (RDFA) has attracted a lot of researchers worldwide in recent years. Depends on different kinds of rare earth ion, RDFA can be categorized into neodymium doped fiber amplifier (NDFA), erbium doped fiber amplifier (EDFA), thulium doped fiber amplifier (TDFA), and so forth. Among many kinds of RDFA, the ytterbium doped fiber amplifier (YDFA) has received even more interest, especially in high power application, mainly because of its broad gain bandwidth and high conversion efficiency which are due to its relatively simple electronic structure.

The purpose of this research is to study the YDFA by developing a model and building a YDFA setup in free space configuration. The active fiber used in the setup is a few modes, polarization-maintaining double-cladding ytterbium-doped large mode area (LMA) fiber and the length is 1m. The pump used is a tunable 975nm laser diode and a 1064nm laser diode was used as the seed which has 630 ps pulse duration time and 9.59 kHz repetition rate. This setup produces 2.514W average power, corresponding to a pulse peak power of 423kW, with 15W absorbed pump power. The spectrum of the output power has also been investigated.

For Victoria.

ACKNOWLEDGEMENTS

First and foremost, I would like to extend my sincere gratitude and appreciation to my advisor, Dr. Rodrigo Amezcua Correa, who has given me the opportunity to work in his group and to work on this research, for providing support and guidance throughout my time in Microstructured Fibers and Devices group. It is impossible to finish this research without him.

Then I would like to deeply thank my committee member, Dr. Axel Schülzgen and Dr. Sasan Fathpour, for their time and essential suggestions.

I would also like to thank Joshua Bradford for answering me many questions when I were building my experiment setup.

I would like to thank all my friends and group mates, for helping me and making my life in CREOL enjoyable.

Finally, I want to express my appreciation to my family and my girlfriend, for their selfless and consistent support in my life. Their help and support was the most important reason why I could overcome all difficulties in the past two years.

TABLE OF CONTENTS

LIST OF FIGURES

LIST OF TABLES

LIST OF ACRONYMS/ABBREVIATIONS

ASE: Amplified Spontaneous Emission

EDFA: Erbium Doped Fiber Amplifier

ESA: Excited State Absorption

LMA: Large Mode Area

LP: Linearly Polarized

NDFA: Neodymium Doped Fiber Amplifier

OSNR: Optical Signal-To-Noise Ratio

PM: Polarization Maintaining

RBS: Rayleigh Backscattering

RDFA: Rare-earth Doped Fiber Amplifier

SPM: Self Phase Modulation

TDFA: Thulium Doped Fiber Amplifier

TIR: Total Internal Reflection

YDFA: Ytterbium Doped Fiber Amplifier

CHAPTER 1: INTRODUCTION

Comparing to traditional bulk optical gain media, rare earth doped fiber is more compact, efficient, mechanical and thermal stable [1]. With such characteristics, amplifiers based on rare earth doped fiber are one of the hottest topics of optics in recent years, and already play a vital role in many commercial applications such as telecommunications, fiber sensing applications, laser sources amplification for medical imaging, and so forth [2], [3]. Although rare earth doped fiber amplifier (RDFA) received a lot of attention in these years, however, the idea that applying optical fiber in laser to reduce required pump power can be dated back to 1961 when E. Snitzer proposed a fiber cavities for optical masers [4]. Unfortunately, because technologies at that time were not advance enough, building a useable RDFA is unrealistic. This situation has changed in 1980s when researcher, who motivated by the application of optical amplifier in fiber optics communication, revisited this topic with advanced fiber fabrication technique and high power laser diode [1]. Since then, RDFA attracted more and more interest, amplifier with different type of rare earth ions and different schemes were introduced one after another. In 1987, the erbium-doped fiber amplifier (EDFA) was presented by R. J. Mears *et al.* [5], later the Thulium doped fiber amplifier (TDFA) and the Praseodymium doped fiber amplifier (PDFA) were introduced for amplification in S-band and 1300nm region respectively. Among all these RDFAs, the EDFA is the most popular one since its amplification region is the one which widely used in optical fiber communication. Thus, it is reasonable that researchers play more attention on EDFAs and

try to apply EDFAs in more applications other than telecommunication. Then researchers started to use EDFAs to gain high peak power laser.

However, in such application, amplifier need to amplify a wide wavelength range of source, which means EDFA's ability to provide amplification on wavelength used in fiber optics communication no longer necessary. In fact, due to excited state absorption, concentration quenching, and relatively low doping level [2], the EDFA is not an ideal amplifier in these kinds of application. Comparing to the EDFA, the ytterbium doped fiber amplifier (YDFA) doesn't have excited state absorption and concentration quenching problem, moreover it can easily reach a high concentration of rare earth ions and has broad gain bandwidth and broad pump wavelength. With so many advantages, YDFAs attracted so much interest and already play an important role on high power application. Also, due to its wide gain bandwidth and broad gain bandwidth, YDFAs are ideal in ultrashort optics application, and can be pump by many different schemes.

After years of rapid development, many different YDFAs have been proposed and a lot of good amplifications have been demonstrated. R.Song *et al*. demonstrated a picosecond laser with 157W average power by using ytterbium double cladding fiber in a threes stages YDFA configuration[7]. J. M. Sousa *et al*. presented a broadband high power diode pumped YDFA with 2.8W average output power [8]. The ytterbium doped fiber they used is a 14m long double cladding fiber with 220µm diameter inner cladding and 7.6µm diameter core. S. Chen and his/her colleagues reported a 100W all fiber picosecond master oscillator power amplifier laser by using three stages YDFA [18]. Between each stage, they applied a bandpass filter to filter out

amplified spontaneous emission (ASE). K. Kieu *et al*. built a high-power picosecond fiber source for coherent raman microscopy which could be used in biological imaging [9]. They used a two stages YDFA scheme, both stages are based on double cladding ytterbium doped fiber and in the main stage, they put fiber in two orthogonal planes to eliminate high order modes. K. Chen *et al.* from university of Southampton demonstrated a linearly polarized picosecond ytterbium doped fiber MOPA with output average power up to 100W [10]. Beside of experiment, many modeling works have been done by researchers, for example Yong Wang *et al.* proposed a theoretical model for double cladding ytterbium doped fiber amplifiers with kilohertz repetition rate nanosecond pulses [11].

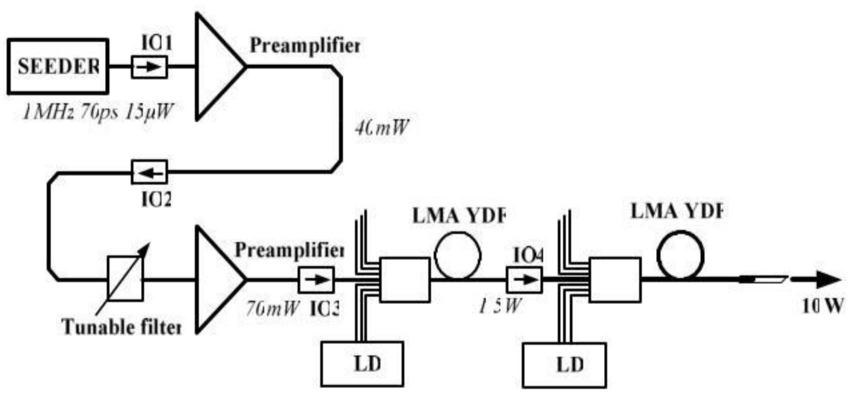

Figure 1: A typical YDFA, this YDFA contain 2 stages of ytterbium doped fiber based main amplifier and 2 stages of preamplifier [12]

The overall purpose of this thesis is to investigate YDFA theoretically and experimentally by building a numerical model and a two-stages YDFA setup. The active fiber used in the experiment is a polarization-maintaining large mode area (LMA) double-clad ytterbium doped

fiber (Nufern PLMA-YDF-25/250-VIII), and the setup is in free space configuration. The output mode is monitored though a CCD camera, both the output spectra and the output average power have been investigated and will be discussed in following chapters.

This thesis is arranged in six chapters. In Chapter 2, theoretical background of this thesis, such as basic knowledge of fiber optics, fabrication of rare earth doped active fiber, pumping scheme, and angle cleaving, are provided. Chapter 3 show how the numerical model is developed and solved though iteration. The experiment setup is presented in detail in Chapter 4. All the measurement result and discussion are reported in Chapter 5. And finally, Chapter 6 will make a conclusion and give some recommendations about how to improve the experiment setup to gain a better result.

CHAPTER 2: THEORTICAL BACKGROUND

2.1 Fiber Optics Basic

Optical fiber is a silica based hair-thick low-loss transmission medium. Although it was originally designed for long distance optical communication, specially designed optical fiber could be used in other applications, for example, optical fiber doped by rare earth ions can be used in fiber amplifier and fiber laser [13]. One of the most important properties of optical fiber is its low-loss characteristic, and this is due to total internal reflection (TIR).

2.1.1 Total Internal Reflection

According to Snell's law,

$$n_1 \sin(\theta_1) = n_2 \sin(\theta_2) \tag{1}$$

where n_1 and n_2 are refractive index of region 1 and region 2 respectively, θ_1 and θ_2 are incident and refractive angel of light, when light from region 1 enter region 2 with incident angel θ_1, light will be refracted with angel θ_2. If we rearrange Snell's law into

$$\theta_1 = \arcsin(\frac{n_2}{n_1} \sin(\theta_2)) \tag{2}$$

clearly when $n_1 > n_2$ and $\theta_2 = 90°$, θ_1 will reach a critical angel θ_c, and if incident angle θ_1 larger than θ_c, all light will be reflected to region 1, no light can transmit into region 2. And this is called total internal reflection (TIR).

2.1.2 Optical Fiber

Structure of optical fiber is showed below:

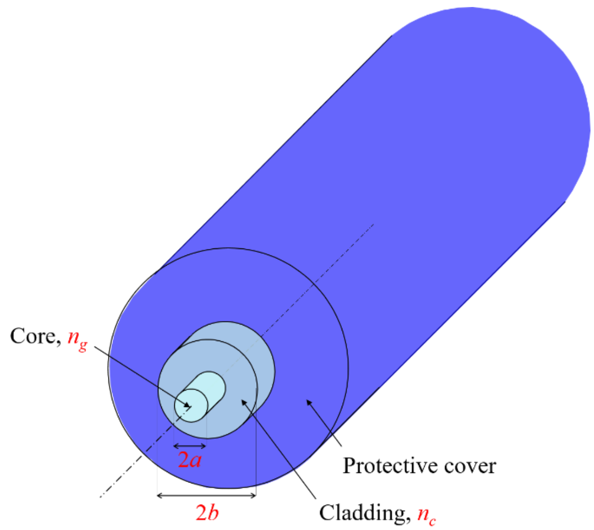

Figure 2: Optical fiber structure

All optical fiber can be divided into three parts: core, cladding, and protective cover. Both core and cladding are based on silica, notice that the refractive index of core (n_g) is larger than refractive index of cladding (n_c). As a result, due to total internal reflection (TIR), light will be trapped inside the core and travel a long distance with limited loss.

One of the most important parameter of optical fiber is numerical aperture (NA), which describe the angle range of incident light that an optical fiber could accept. Due to Snell's law and total internal reflection (TIR), we can easily prove that only light with incident angel that

within the fiber acceptance angel can meet the TIR requirement and be guided inside optical fiber core. NA can be described by the following equation:

$$\mathrm{NA} = \mathrm{n}\sin(\theta_{\mathrm{max}}) = \sqrt{\mathrm{n_g^2} - \mathrm{n_c^2}} \tag{3}$$

where n is the refraction index of the medium that incident light come from. θ_{max} is the maximum acceptance angle of optical fiber, n_g and n_c are refraction index of fiber core and cladding respectively.

2.1.3 Linear Polarized Modes

In cylindrical waveguide, only certain modes can travel inside, and these modes are HE_{lm} or EH_{lm} modes. However, most optical fibers are in weakly guide regime where $\Delta = \frac{n_1 - n_2}{n_1} \ll 1$, and in this regime HE_{lm} and EH_{lm} modes become degenerate. And these degenerate modes are categorized into different linear polarized (LP) modes.

Table 1: HE_{lm} and EH_{lm} modes categorized into LP modes

LP mode	Traditional mode	Degeneracy
LP_{01}	HE_{11}	2
LP_{11}	$HE_{21}\times2, TE_{01}, TM_{01}$	4
LP_{21}	$HE_{31}\times2, EH_{11}\times2$	4
LP_{02}	$HE_{11}\times2$	2
LP_{31}	$HE_{41}\times2, EH_{21}\times2$	4

Some examples of LP modes are shown in Figure 3.

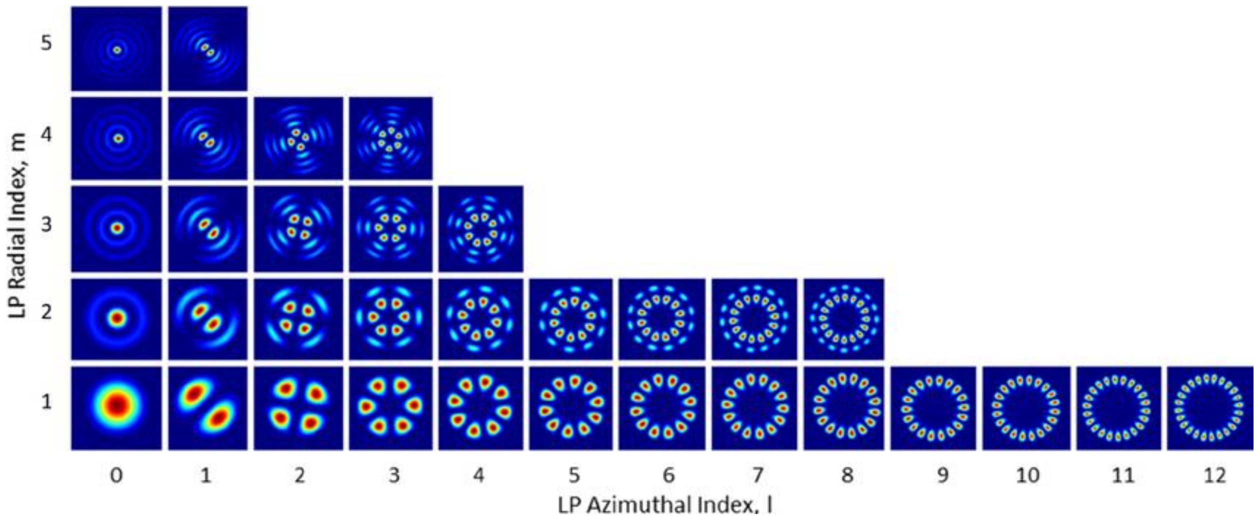

Figure 3: Example of LP modes [14]. The LP mode on the bottom left corner is LP_{01} mode

2.1.4 Angel Cleaving

According to the law of reflection, if the fiber end is cleaved at 90 degrees, reflected light will still fulfill the TIR and be guided to the other end of fiber. This would cause a problem in YDFA, since the reflected light would be amplified again in the active fiber and this would turn the active fiber into a laser cavity. Since what we want is an amplifier not a laser, certainly we need to avoid this problem. To do so, we can limit the amount of reflected light that fulfill TIR by cutting the fiber end at an angel different from 90 degrees. Such process called angel cleaving. Notice that not every fiber cleaver could be able to do angel cleaving, the one we used in here is vytran's LDC-400.

Figure 4: vytran's LDC-400 cleaver. Source: vytran.

2.1.5 Polarization Maintaining Optical Fiber

In some application, it is essential to maintain the linear polarization of linear polarized input light while it's going through optical fiber. To do so, a special kind of optical fiber called polarization maintaining (PM) optical fiber has been developed. The principle of PM optical fiber is simple. Stress can modify atom placement which will affect the phase velocity of light. Thus, we could place stress rod inside the fiber and such stress rod can increase the stress along the line of the rod. Then the polarization parallel to the stress rod would have phase velocity that different from the perpendicular one, and as a result the polarization of the input light could be maintained. There are serval different kinds of design of PM optical fiber such as panda type, bow-tie type, and elliptical type. These different kinds of PM optical fiber are shown below:

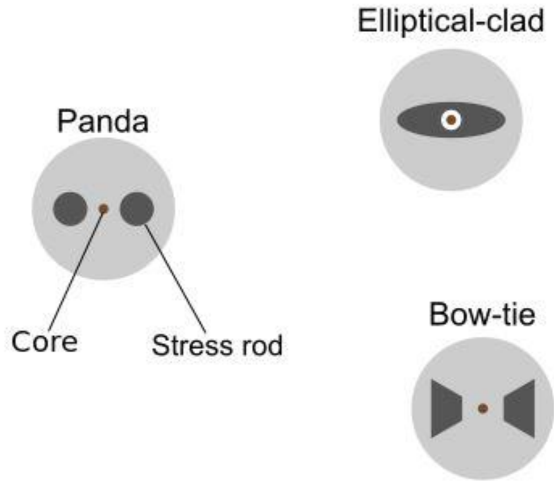

Figure 5: Different types of PM optical fiber. Credit: Bart133

2.2 Fundamental of Ytterbium Doped Fiber Amplifier

In this part, some basic yet important knowledge about YDFA would be presented. This knowledge should be very helpful for understanding the following chapter.

2.2.1 Principle of Laser

According to Einstein's theory, there are three main processes occurring in the active medium during radiation: spontaneous emission, absorption, and stimulated emission. As there name imply, spontaneous emission means atoms in state 2 could decay to state 1 spontaneously, absorption means atoms in state 1 absorb photons and then convert to state 2, simulated emission means atoms in state 2 emit photons and return to state 1. Notices that the photon emitted through stimulated emission are at the same frequency, in the same polarization, in the same

direction, and in the phase of the stimulating wave. Figure 6 show a simplified scheme with only two energy levels of these three process:

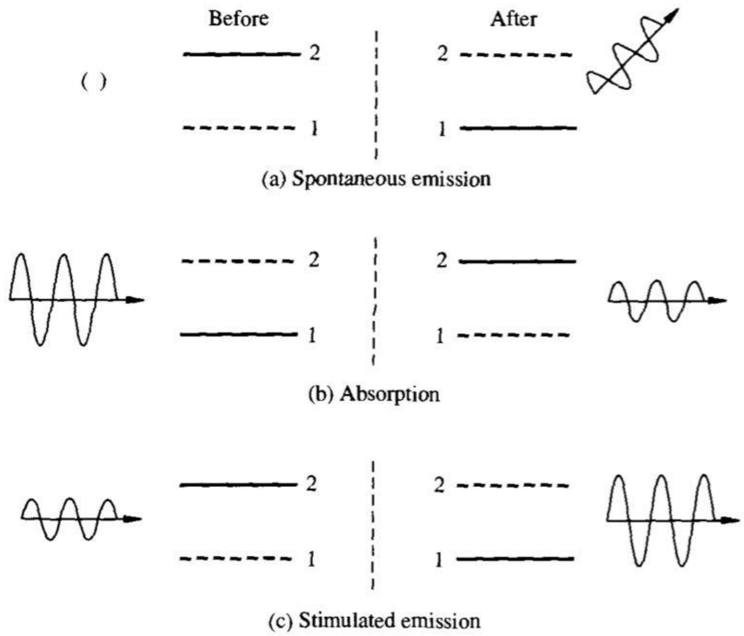

Figure 6: Simplified scheme of three main processes occurring in active medium [15]

Normally, most atoms in active medium are in the ground state, as a result, no spontaneous nor stimulated emission happen which means no photon is emitted. However, if the medium is pumped hard enough, population inversion would happen, highly coherent photons would be emitted thought stimulated emission. If this active medium is inside a resonator cavity which can provides optical feedback, those emitted photons could be amplified again and again and finally yield a highly coherent laser light.

2.2.2 Spectroscopic Properties of Ytterbium

Comparing to other rare earth ion, ytterbium's spectroscopy is relatively simple: two level manifolds can account for all wavelengths. These two manifolds are $2_{F_{7/2}}$ and $2_{F_{5/2}}$, each contain 4 and 3 sublevels respectively. Energy level diagram of these two manifolds are shown in Figure 7.

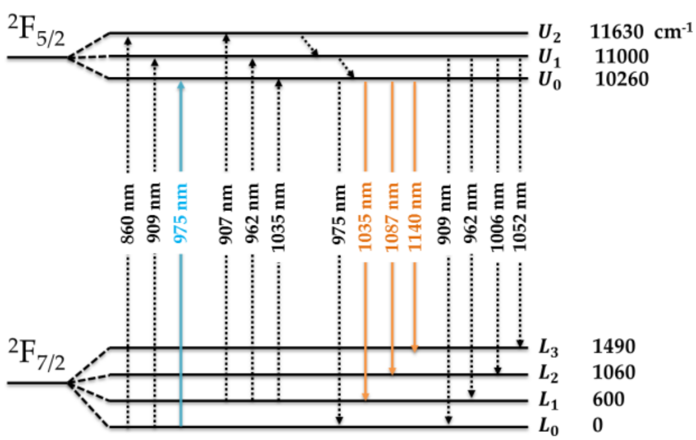

Figure 7: Energy level diagram of $2_{F_{7/2}}$ and $2_{F_{5/2}}$ [16]

The absorption and emission cross sections of ytterbium-doped silica optical fiber are presented in Figure 8. Notice that the host glass composition could affect the absorption and emission cross section spectra in some extent [2].

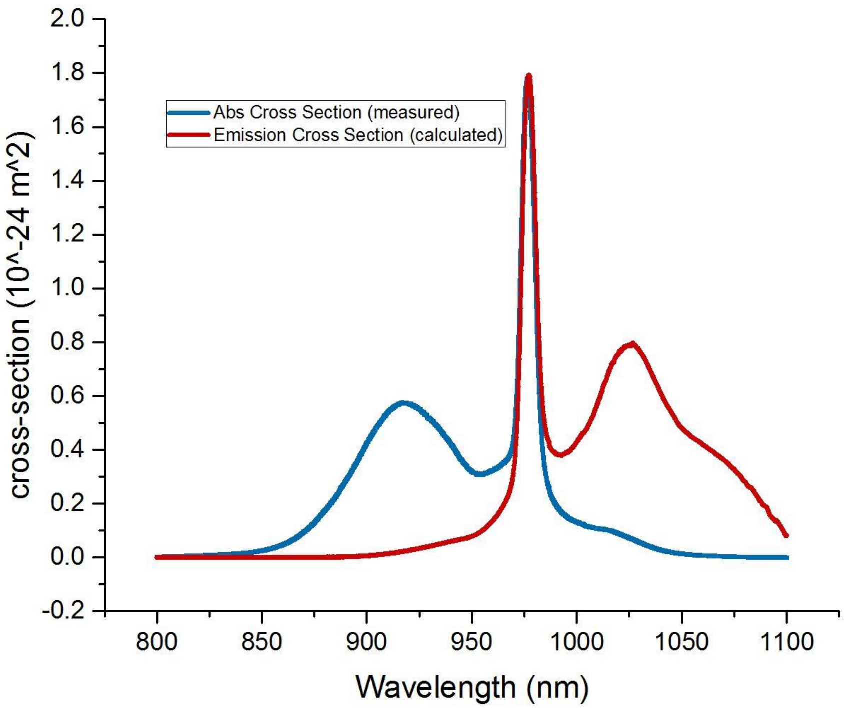

Figure 8: Absorption and emission cross section of ytterbium-doped silica optical fiber. Source: Nufern

2.2.3 Ytterbium Doped Optical Fiber

As its name implies, Ytterbium doped optical fiber is a kind of active fiber that doped with ytterbium ions. These ytterbium ions introduce energy levels to the fiber so that the optical fiber could interact with input pump light. Just like ordinary gain medium in other laser system, three processes occur in the active fiber: spontaneous emission, absorption, and stimulated emission, and if the power of pump light high enough, population inversion would begin and active fiber would turn in optical amplifier or fiber laser. Notice that photons emitted thought spontaneous emission could also be amplified in active fiber, and this is called amplified spontaneous emission (ASE). ASE would consume a proportion of pump energy which could be

used to amplifier input signal light, which means ASE could reduce the overall gain of seed light. To suppress the impact of AES, we could insert a bandpass filter between each stage to filter out ASE or use a double-pass configuration so that the signal could be amplified twice while ASE only be amplified once [2]. Methods to suppress ASE would be discuss in detail in Chapter 4.

2.2.4 Cladding Pumping and Double Cladding Optical Fiber

In term of beam quality, single mode optical fibers are always good choice. However, in high power application, using a single mode fiber is inefficient. Because most high-power light source emit multi-mode light, and coupling between multi-mode light and single mode fiber is quite inefficient. Also, the relatively small core size of single mode fiber will also limit the coupling efficiency and require very precise alignment, since most high-power light source have a large spot size. This problem could be tackle by implement double-cladding optical fiber, which is first demonstrated by Snitzer *et al.* in 1980s [17]. As its name implies, double-cladding fiber contains two cladding: outer and inner cladding. The refraction index of inner cladding is between outer cladding and core, so that multi-mode high power light could travel in inner cladding while the signal light could travel in the core. There many geometries of inner cladding, the one used in here is a polarization maintaining double cladding fiber, its cross section is shown in Figure 9.

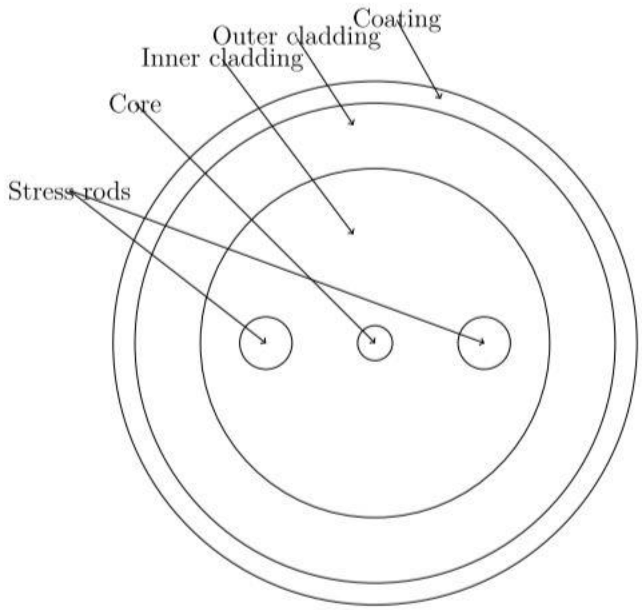

Figure 9: Cross section of the double cladding fiber used in following experiment [21]

By using double-cladding optical fiber, one can combine the advantage of single mode fiber and the advantage of multi-mode fiber: signal could be coupled to single mode core to obtain good beam quality, at the same time, high power pump light could be couple to multi-mode inner cladding efficiently. Such scheme is called cladding pumping. Notice that in rare earth doped double cladding fiber, rare earth ions only exist in the core, however, modes of the inner cladding have some overlap with the core so that high power light could be absorbed [2]. Nowadays, double cladding fiber and cladding pumping have been used in many RDFA, active fiber in [3, 18, 19] are all double cladding fiber.

CHAPTER 3: MODELING

There is no doubt that model is much simpler than reality. Meanwhile, reality is way too complicate for human being to understand. As a result, people use model, which is simple enough to be handle by people, to have a glance on reality, to understand certain aspects of the real world.

In this chapter, a numerical model of YDFA based on rate equations is developed and solved thought four-order Runge-Kutta method and iteration. In order to simplify the model, monochromatic, continuous wave pump and seed are assumed, the effect of amplified spontaneous emission (ASE) is included but nonlinear effects as well as excited state absorption (ESA) aren't considered. What's more, we reduced the three-level system into the two-level system [20].

3.1 Rate Equation

The local ytterbium ion population of upper state and ground state can be described by rate equations:

$$\frac{dn_2}{dt} = (R_{12} + W_{12})n_1 - (R_{21} + W_{21} + A_{21})n_2 \tag{4}$$

$$n_t = n_1 + n_2 \tag{5}$$

Where n_1, n_2, and n_t are ytterbium ion population of ground state, upper state, and both states respectively. R_{12} and R_{21}represent transition rates relative to pump, W_{12} and W_{21} are transition

rates relative to seed, and $A_{21}$is the spontaneous emission rate. These five parameters are governed by equation (6) - (10):

$$R_{12} = \frac{\sigma_a(\lambda_p)\lambda_p}{hc} I_p \quad (6)$$

$$R_{21} = \frac{\sigma_e(\lambda_p)\lambda_p}{hc} I_p \quad (7)$$

$$W_{12} = \frac{\sigma_a(\lambda_s)\lambda_s}{hc} I_s \quad (8)$$

$$W_{21} = \frac{\sigma_e(\lambda_s)\lambda_s}{hc} I_s \quad (9)$$

$$A_{21} = \frac{1}{\tau} \quad (10)$$

Where $\sigma_a(\lambda_p)$ and $\sigma_a(\lambda_s)$ are absorption cross sections of pump and seed respectively, $\sigma_e(\lambda_p)$ and $\sigma_e(\lambda_s)$ are emission cross section of pump and seed correspondingly, and τ is the life time of upper state. I_p and I_s are pump and seed intensities. Notice that not all pump and seed power can be absorbed by the active fiber. In order to describe the proportion of pump or seed that are absorbed by the fiber, we introduce overlap factor: Γ_s for seed and Γ_p for pump, so that I_s and I_p can be described by:

$$I_{s/p} = \Gamma_{s/p} \frac{P_{s/p}}{A} \quad (11)$$

Where A denotes the doped area of the active fiber.

Also, we need to realize that n_1 and n_2 are vary in different longitudinal position (z) of the fiber, so they should be denoted as $n_1(z,t)$ and $n_2(z,t)$. Putting equations (6) – (11) into equation (4), we have:

$$\frac{dn_2(z,t)}{dt} = \frac{\Gamma_p \lambda_p}{hcA}\left[\sigma_a(\lambda_p)n_1(z,t) - \sigma_e(\lambda_p)n_2(z,t)\right].P_p - \frac{n_2(z,t)}{\tau} +$$

$$\frac{\Gamma_s \lambda_s}{hcA}\left[\sigma_a(\lambda_s)n_1(z,t) - \sigma_e(\lambda_s)n_2(z,t)\right].P_s \qquad (12)$$

The power propagation varies in wavelength, which means we have different equations for pump and seed:

$$\frac{dP_p}{dz} = \Gamma_p\left(\sigma_e(\lambda_p)n_2(z,t) - \sigma_a(\lambda_p)n_1(z,t)\right)P_p - \alpha P_p \qquad (13)$$

$$\frac{dP_s}{dz} = \Gamma_s\left(\sigma_e(\lambda_s)n_2(z,t) - \sigma_a(\lambda_s)n_1(z,t)\right)P_s - \alpha P_s \qquad (14)$$

Where α is the fiber background losses.

Obviously, form equations (13) and (14), we can clearly realize that the power also vary in time, thus these two equations should be rewrite into:

$$\frac{\partial P_p}{\partial z} + \frac{1}{\nu_p}\frac{\partial P_p}{\partial t} = \Gamma_p\left(\sigma_e(\lambda_p)n_2(z,t) - \sigma_a(\lambda_p)n_1(z,t)\right)P_p - \alpha P_p \qquad (15)$$

$$\frac{\partial P_s}{\partial z} + \frac{1}{\nu_s}\frac{\partial P_s}{\partial t} = \Gamma_s\left(\sigma_e(\lambda_s)n_2(z,t) - \sigma_a(\lambda_s)n_1(z,t)\right)P_s - \alpha P_s \qquad (16)$$

Where ν_p and ν_s are group velocity of pump and seed correspondingly.

Up until now, we haven’t taken ASE in to account, thus in this following part ASE will be considered and both rate equations and power propagation equations will be modified.

3.2 Considering Amplified Spontaneous Emission

The spontaneous emission coefficient $A_{21} = {}^{1}\!/_{\tau}$ can describes the rate of ions in upper state emit photons spontaneously. Thus A_{21} along with photon energy could represent spontaneous power:

$$P_{se} = \frac{hf}{\tau} \tag{17}$$

Where f is the frequency. Also, we introduce line shape function, thus the probability that the spontaneous emission happen in a frequency range is: $\mathrm{g}(\mathrm{f} - f_0)\Delta\mathrm{f}$. We use frequency range here because we need to simplify the calculation then divide the whole ASE spectrum into several channels, each channel has a width of Δf. What's more, since the total spontaneous emission power depend on the population of upper state ions, the total spontaneous emission, also known as ASE, can be described as:

$$\mathrm{g}(\mathrm{f} - f_0)\Delta\mathrm{f}\frac{hf}{\tau} n_2(z,t)\pi r^2 \tag{18}$$

where r is the core radius. Besides, we realize that only a portion of ASE fulfill the guiding requirement of fiber, as a result, we introduce a parameter F, to represent such fraction and equation (18) turn into:

$$\mathrm{g}(\mathrm{f} - f_0)\Delta\mathrm{f}\frac{hf}{\tau} n_2(z,t)\Gamma_s F\pi r^2 \tag{19}$$

After using the relation introduced in [21-23], and apply Δλ instead of Δf, we finally obtained the ASE expression of each channel:

$$P_{ASE} = 2\sigma_e(\lambda)\Gamma_s n_2(z,t)\frac{hc^2\Delta\lambda}{\lambda^3} \tag{20}$$

3.3 Rate Equations with ASE Term

In this thesis, we only use forward pumping, thus pump power could only propagate forward. We combine equation (12), (15), (16), and (20) together, consider all channels and the fact that ASE could propagate forward or backward. Optimized rate equations are shown below:

$$\frac{dn_2(z,t)}{dt} = \frac{\Gamma_p\lambda_p}{hcA}\left[\sigma_a(\lambda_p)n_1(z,t) - \sigma_e(\lambda_p)n_2(z,t)\right].P_p - \frac{n_2(z,t)}{\tau} +$$

$$\frac{\Gamma_s}{hcA}\sum_{k=1}^{K}\lambda_k[\sigma_a(\lambda_k)n_1(z,t) - \sigma_e(\lambda_k)n_2(z,t)]\cdot[P_k^+ + P_k^-] \tag{21}$$

$$n_t = n_1(z,t) + n_2(z,t) \tag{22}$$

$$\frac{\partial P_p}{\partial z} + \frac{1}{v_p}\frac{\partial P_p}{\partial t} = \Gamma_p[\sigma_e(\lambda_p)n_2(z,t) - \sigma_a(\lambda_p)n_1(z,t)]P_p - \alpha P_p \tag{23}$$

$$\pm\frac{\partial P_k^\pm}{\partial z} + \frac{1}{v_s}\frac{\partial P_k^\pm}{\partial t} = \Gamma_s[\sigma_e(\lambda_k)n_2(z,t) - \sigma_a(\lambda_k)n_1(z,t)]P_k^\pm - \alpha P_k^\pm +$$

$$2\sigma_e(\lambda_k)\Gamma_s n_2(z,t)\frac{hc^2\Delta\lambda}{\lambda_k^3}, k = 1, \dots \mathrm{K} \tag{24}$$

Where $P_k^\pm$ denotes the forward or backward power of channel k.

3.4 Solving the Rate Equation

In order to simplify the calculation, we solve the rate equation in steady state, which's mean we let $\frac{dn_2(z,t)}{dt} = 0$. Along with equation (21) and (22), we gain the expression for $n_2(z)$ in steady state:

$$n_2(z) = \frac{(\frac{\Gamma p \lambda p}{hcA}\sigma_a(\lambda_p)P_p + \frac{\Gamma_s}{hcA}\sum_{k=1}^{K}\lambda_k\sigma_a(\lambda_k)\cdot[P_k^+ + P_k^-])n_t}{\frac{\Gamma p \lambda p}{hcA}P_p\left(\sigma_e(\lambda_p)+\sigma_a(\lambda_p)\right)+\frac{\Gamma_s}{hcA}\sum_{k=1}^{K}\lambda_k\left(\sigma_e(\lambda_k)\cdot+\sigma_a(\lambda_k)\right)\cdot[P_k^+ + P_k^-]+\frac{1}{\tau}} \tag{25}$$

Meanwhile, in steady state, power distribution inside the active fiber no longer change in time, as a result, equation (23) and (24) could be simplified into:

$$\frac{\partial P_p}{\partial z} = \Gamma_p[\sigma_e(\lambda_p)n_2(z) - \sigma_a(\lambda_p)n_1(z)]P_p - \alpha P_p \tag{26}$$

$$\pm\frac{\partial P_k^\pm}{\partial z} = \Gamma_s[\sigma_e(\lambda_k)n_2(z) - \sigma_a(\lambda_k)n_1(z)]P_k^\pm - \alpha P_k^\pm +$$

$$2\sigma_e(\lambda_k)\Gamma_s n_2(z)\frac{hc^2\Delta\lambda}{\lambda_k^3}, k = 1, \dots \mathrm{K} \tag{27}$$

Obviously, equation (26) and (27) are first order ordinary differential equations, however, to get exact solution of these equations is time consuming. As a result, in this thesis we only get the approximated solution by using fourth-order Runge-Kutta method which is also known as RK4.

The usage of RK4 is shown below. Here are a first order differential equation and its initial condition:

$$\begin{cases} \frac{dy}{dt} = f(t,y) \\ y(t_0) = \alpha \end{cases} \tag{28}$$

To approximate the solution of y through RK4, we introduce a parameter: time step h and then $t_{i+1} = t_i + h$. After that, we have:

$$\begin{cases} w_0 = \alpha \\ k_1 = hf(t_i, w_i) \\ k_2 = hf(t_i + \frac{h}{2}, w_i + \frac{k_1}{2}) \\ k_3 = hf(t_i + \frac{h}{2}, w_i + \frac{k_2}{2}) \\ k_4 = hf(t_i + h, w_i + k_3) \end{cases} \quad (29)$$

$$w_{i+1} = w_i + \frac{1}{6}(k_1 + 2k_2 + 2k_3 + k_4) \quad (30)$$

Where w_i is the approximation of y(t_i), and with $w_i$we can determine w_{i+1} by using equation (29) and (30). The time step h will determine resolution and the quality of approximation. With smaller h, we can get better resolution, better quality yet required more calculation.

Before implying RK4, we need to tackle the boundary conditions first. Equation (29) shows that we first need to know the initial value, which is the boundary condition of the system. In this thesis, as we mentioned above, we use a forward pumping scheme. Thus, at z=0, the power of pump and signal are the launched pump and signal power. However, we don't know the power of forward and backward ASE at z=0. What we know is that power backward ASE reach its maximum at z=0, where power of forward ASE is zero.

To tackle this problem, we imply an iteration method. The first step of this method is to ignore the power of backward ASE and do the RK4 from z=0 to z=L, where L is the length of active fiber. After that, we will have a set of value of pump power, signal power and forward ASE power. We take their value at z=L, and set backward ASE power at z=L to zero, and with

these value, we do the RK4 from z=L to z=0. After these two RK4, we have a set of value of of pump power, signal power, forward and backward ASE power.

Obviously, these value is not accurate. Because of the ignorance of backward ASE at z=0, power of pump, signal, and forward ASE are larger than their actual value. Thus, after doing the “reverse” RK4, power of backward is underestimated. In order to reach an acceptable result, iteration need to be done, which’s mean do the RK4 and the “reverse” RK4 again and again until the acceptable accuracy (i.e. difference between successive result is less than 10E-7 [24]) is obtained. The flowchart is shown in Figure 10.

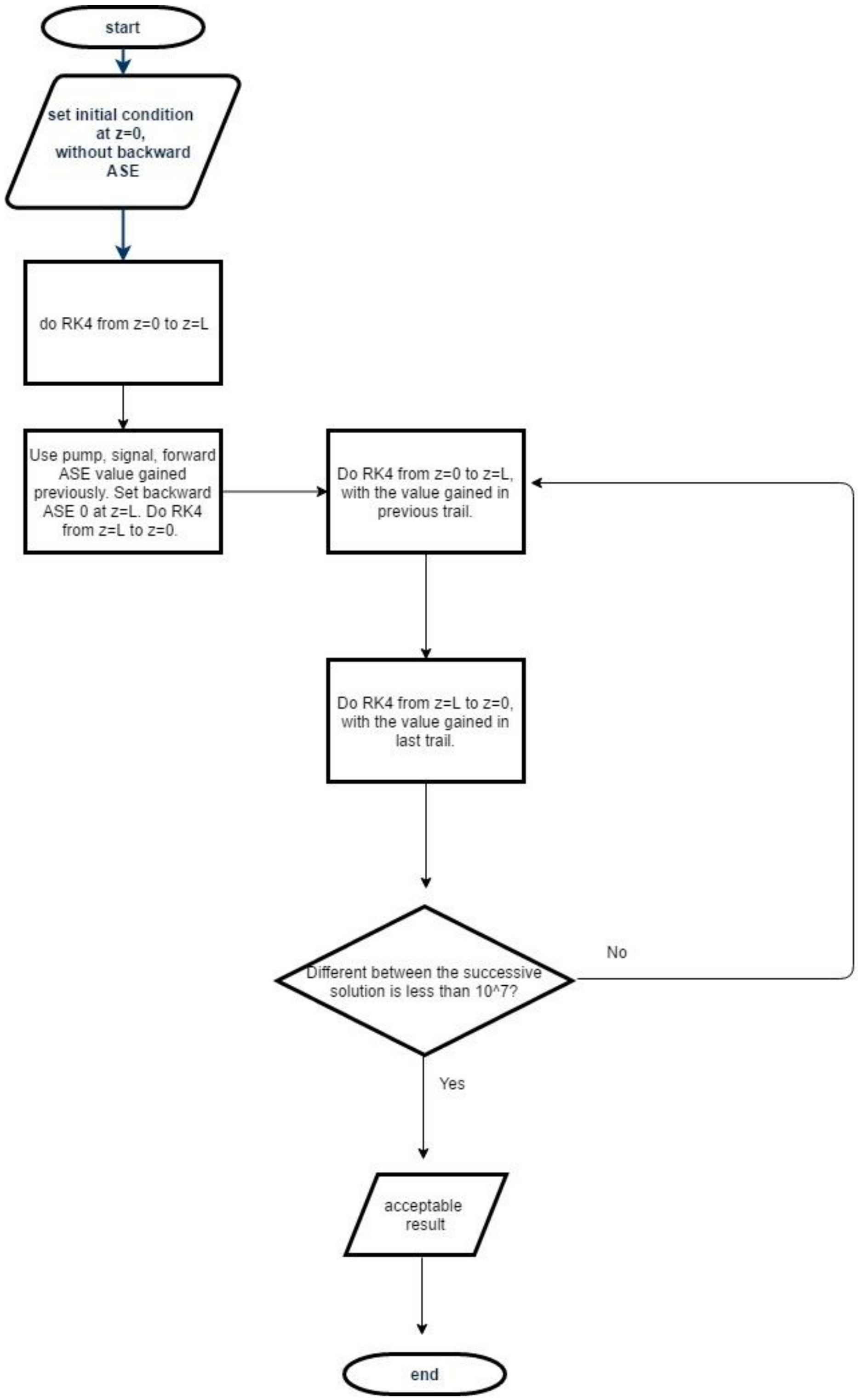

Figure 10: Flowchart of method used to solve rate equations.

3.5 Simulation Result

We wrote the model in MATLAB, and before running the model, we need to specify parameters we used. The wavelength of seed and pump light is 1064nm and 975nm respectively. The ytterbium doped fiber is Nufern's PLMA-YDF-25/250-VIII, its 25μm core and 250μm cladding gives 0.01 overlap factor of the pump, meanwhile we assume that the overlap factor of seed is 0.85. Instead of doping concentration, Nufern only provide the absorption at 975nm, which is 5.1dB/m (1.175m^{-1}). However, doping concentration could be calculated, which is equal to absorption / (overlap factor*absorption cross-section). According to the absorption/emission cross-section data from Nufern, the absorption cross-section at 975nm is 1.65E-24. As a result, the doping concentration is 7.12E25 ion/m^3). In term of absorption/emission cross-section, the absorption/emission cross-section of seed and pump light are 0.0064E24, 0.3978E24, 1.6E24, and 1.5193E24 respectively. What's more, life time of the upper state is set to 860μs, the fiber length is set to 1m, the fiber background loss is set to 0.25dB/km, the doped area is 6.25E-10m^2.

As we mentioned above, ASE need to be calculated in many channel and each channel has the same bandwidth. However, in order to simplify the calculation, we apply effective bandwidth [25-26], which is 233.129nm and centered in 1030nm.

The simulation result is shown below:

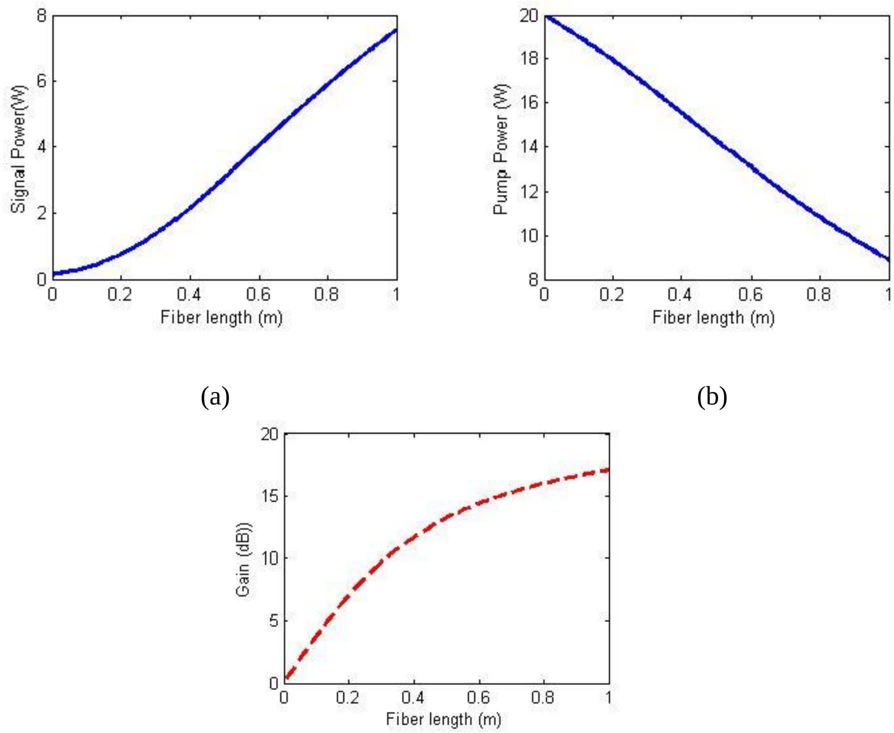

(a) (b)

(c)

Figure 11: Simulation result of 20W pump power and 148mW input seed power (a) output seed power versus fiber length (b) output pump power versus fiber length (c) signal gain versus fiber length.

Figure 11 (a) and (b) show that the power of pump was indeed transfer into the seed. Output power of seed is 7.534W and the output of pump is 8.881W, which's mean 11.119W of pump is absorbed. As a result, the efficiency is 67.8%.

We also investigate the ion population density in upper and ground state. The result is shown in Figure 12.

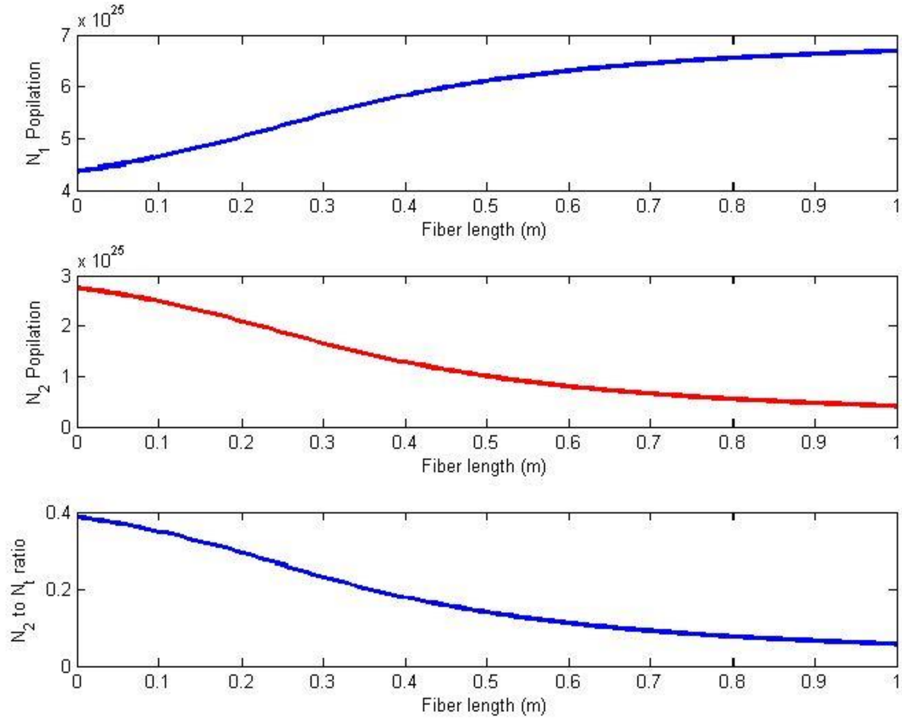

Figure 12: Start from the top, is ground state population density versus fiber length, upper state population density versus fiber length and upper state population to total ion population ratio versus fiber length.

As we mentioned above, we only apply forward pump, which's mean both pump and seed are launched in the same end of active fiber. Figure 12 show that the ion population density of upper state reach its maximum at z=0, at where population density of ground state reach its minimum. That's because z=0 is the point where has maximum pump power and minimum seed power.

Since we pump at 975nm, where absorption and emission cross section are the same, we should get a 50% maximum upper state population to total ion population ratio. However, Figure 12 shows that the maximum ratio we get is just 40%, that is because the power of the pump is

not high enough [2]. Figure 13 shows us that with a higher pump power, for example 60W, the maximum ratio is much closer to 50%.

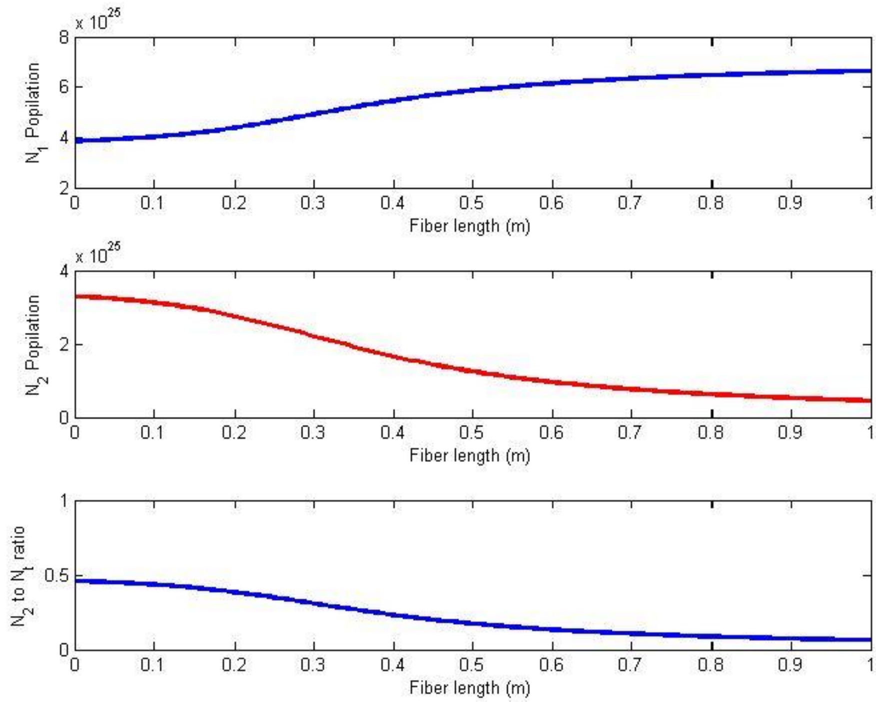

Figure 13: ion distribution along fiber with 60W input pump power and 148mW input signal power

In addition, output seed power versus absorbed pump power is also investigated with the same 148mW input seed power and the result is shown in Figure 14. Figure 14 shows that the output seed power increases with the increasing absorbed pump power consistently. Fitting of the data shows that the slope efficiency is 71.6%.

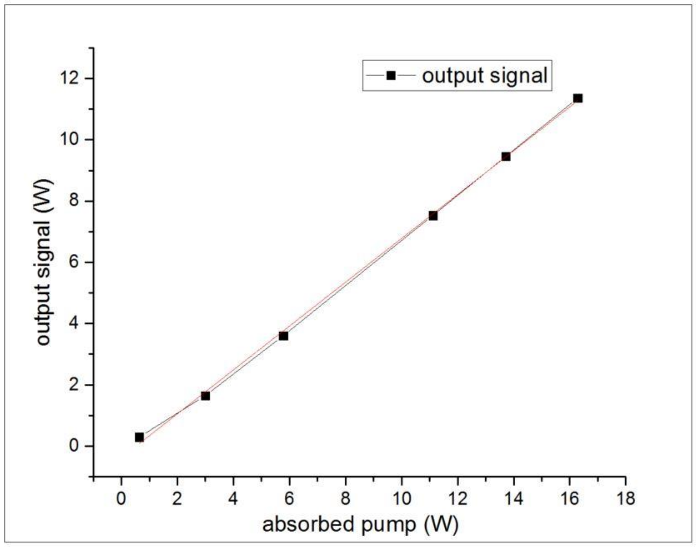

Figure 14: output seed power versus absorbed pump power

CHAPTER 4: EXPERIMENT

4.1 Explanation of Setup

The experiment setup is illustrated in Figure 15. A laser diode (Teem's MNP-06E-000) is used as the seed source and it produces 1064nm seed with 9.59 kHz repetition rate and 620ps duration time. Both ends of two active fibers have been angle cleaved.

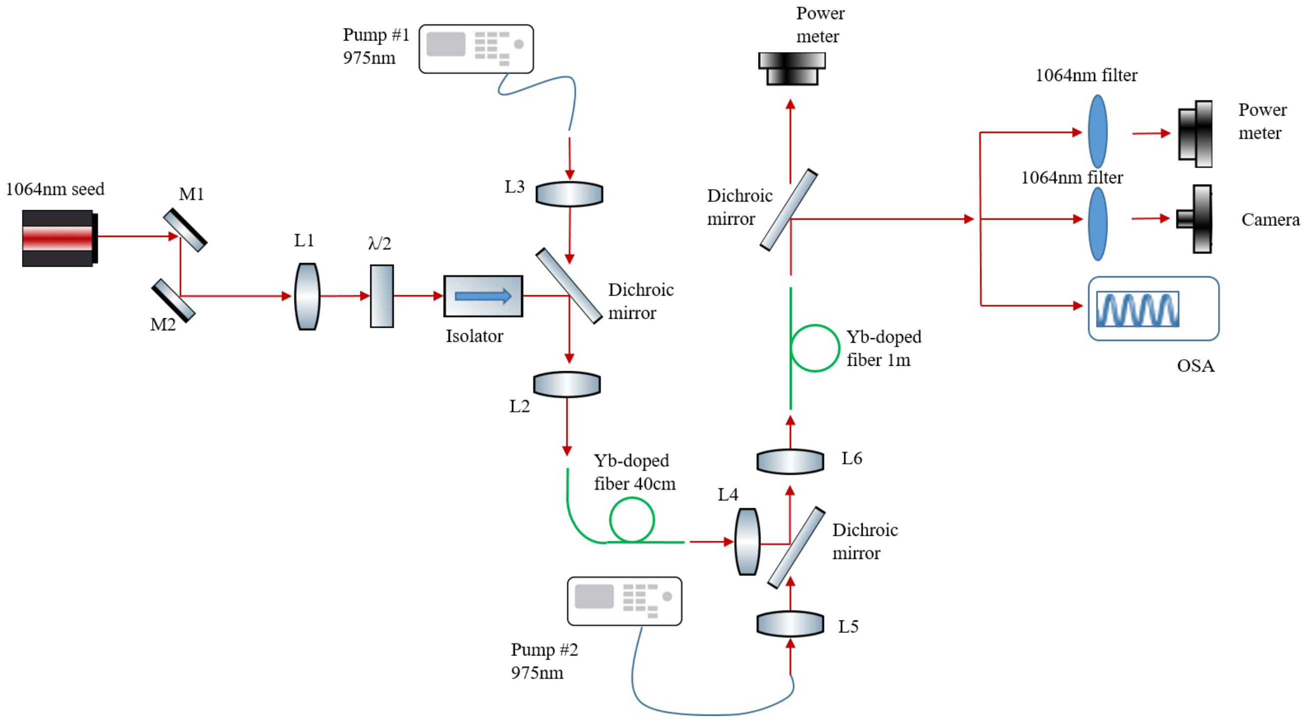

Figure 15: Our YDFA experiment setup.

Since the output direction of the laser diode is fixed, we use two mirrors (M1 and M2) to redirect the seed. The redirected seed is then collimated thought a lens, L1 with 2 inchs focal length and after that it will go through a half-wave plate and an isolator. The half-wave plate

used here is to align the polarization of seed with our free space isolator (IO-F-1064APC), so that we could minimum the loss introduced by isolator. A dichroic mirror (high transmission for 975nm and high reflection for 1064nm) is placed after the isolator, so that our 1064nm seed could be reflected into to L2 (11 mm) and then be coupled into a 40cm long active fiber (Nufern's PLMA-YDF-25/250-VIII)'s core. Meanwhile, 975nm pump light from our pump #1 (BWT's DS3-11322-0113) is coupled into the same 40cm long active fiber's cladding through L2 and L3 (8mm). Since the dichromic mirror has high transmission at 975nm, pump light could go through this mirror with limited loss. The output of 40cm active fiber is then coupled into a 1m long active fiber (Nufern's PLMA-YDF-25/250-VIII) through a pair of lens: L4 and L6 with 4.7mm and 4.6mm focal lengths respectively. The same dichromic mirror as the one mentioned before is placed between L4 and L6. As a result, amplified seed could be reflected to L6 while unabsorbed pump will go through dichromic mirror. Also, pump light from pump #2 (nLight's element e6) is coupled into the same 1m active fiber through L5 and L6. Notice that the focal lengths of L5 is 8mm.

At the other end of our 1m active fiber, we placed another identical dichromic mirror to separate the unabsorbed pump and amplified seed. Unabsorbed pump will be monitored by a power meter, so that we could estimate the coupling efficiency and absorbed pump power. At the meantime, amplified seed would be reflected and be monitored through a power meter, a CCD camera, or a OSA. Power meter is used to monitor average power of output amplified seed, while the spatial mode of output seed would be investigated by the CCD camera. in addition, the spectrum of the output seed is also investigated through a OSA. Notice that, when we monitoring

average power or spatial mode, a 1064nm bandpass filter (Thorlabs' FL1064-10) will be applied to remove the remnant pump power and ASE power.

4.2 Experiment Result

Before amplifying the seed, we first need to estimate the coupling efficiency of the pump so that we could estimate the amount of absorbed pump power. To do so, we only turn on the pump source and measured the output pump power with different launched pump power. Since we know that the absorption at 975nm is 5.1dB/m (Nufern's data), we calculated the actual coupled pump power from output power. As a result, by averaging the calculated coupling efficiency from different launched power, we estimated the coupling efficiency of both pump, which are 93.5% and 66.3% respectively.

Since we used two active fiber here: the 40cm one and the 1m one, we separate our YDFA into two stages. We call the stage with 40cm active fiber the first stage, which is served as preamplifier, and call the stage with 1m active fiber the main stage. Before investigating the average power, we first checked the spatial mode of output seed and the result is shown below. Figure 16 clearly shows that a LP_{01} mode was maintained during the amplification.

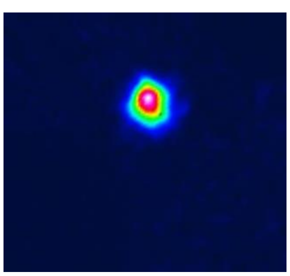

(a)

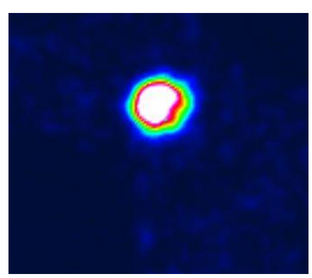

(b)

Figure 16: spatial mode of output seed. (a) is mode of unamplified seed and (b) is mode of amplified seed with 1.4W average power.

As we mentioned above, the 40cm active fiber part is served as the preamplifier. Before being launched into the 1m active fiber, the seed power is amplified to 310mW. After that, we measured the output seed power and output unabsorbed pump power under different launched pump #2 power. In each case, we estimated the actual absorbed pump power. Figure 17 shows that with 15W absorbed pump power, 2.514W seed power has been measured and the gain was 9.09bB.

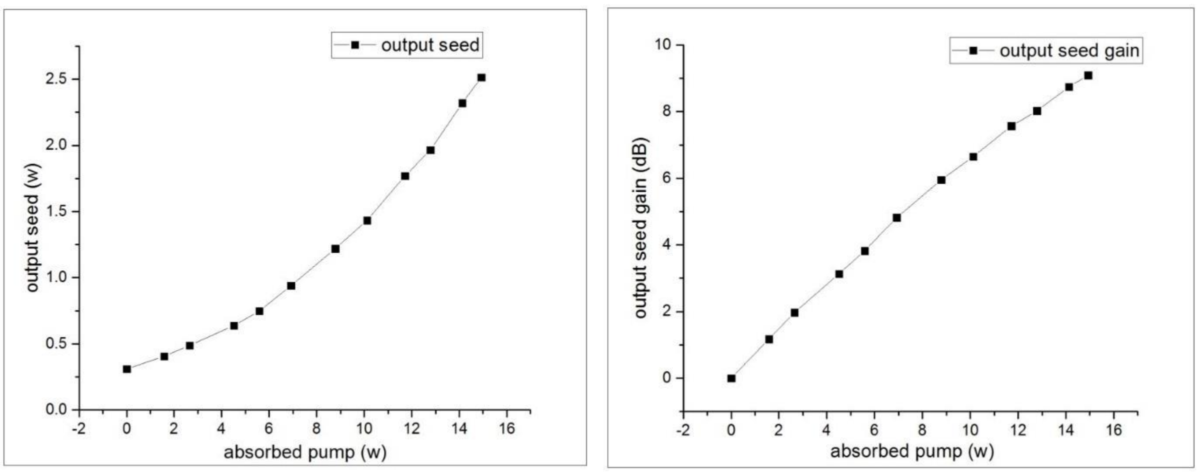

(a) (b)

Figure 17: (a) output seed power versus absorbed pump power. (b) gain of seed versus absorbed pump power.

We notice that even with 15W absorbed pump power, the seed power still has no sign of saturation, which's mean we could gain a higher seed power by increasing the pump power. The seed we used has 9.59 kHz repetition rate and 620ps duration time, as a result, by using equation (31) and (32), we calculated the peak power of the amplified seed, which is 423kW.

$$P_{\text{avg}} = \frac{E}{T} = E \times f \tag{31}$$

$$P_{\text{peak}} = \frac{E}{\Delta t} \tag{32}$$

Where P_{avg} and P_{peak} are average and peak power of seed respectively, f and Δt are repetition rate and duration time respectively. Also, through linear fitting, we also obtained the slope efficiency of our amplifier, which is 15%. Obviously, comparing to the simulation result mentioned before, slope efficiency from experiment is too low. This problem will be discussed detailly later.

In order to investigate the output signal carefully, we also measured the output spectrum through OSA. To do so we first need to remove the 1064nm bandpass filter. The output spectrum under different pump power is shown in Figure 18.

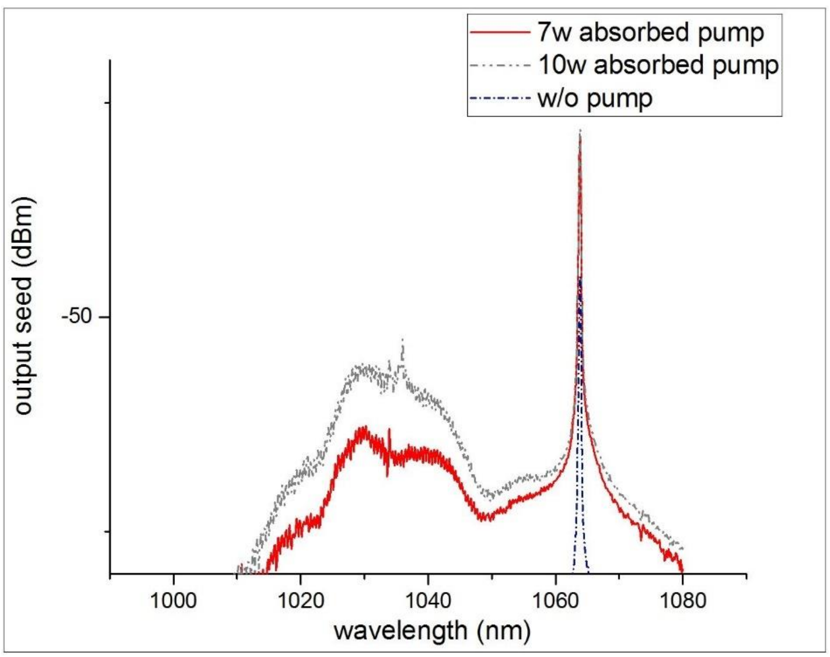

Figure 18: output signal spectrum under different absorbed pump power.

Figure 18 shows that along with the growth of 1064nm seed, a significant growth of ASE that centered at 1030nm also has been observed. With 7W absorbed pump power, the Optical Signal-To-Noise Ratio (OSNR) was up to 34dB, however, when the absorbed pump power was increased to 10W, the OSNR decreased to 24bB. This is because there is an emission cross section peak at 1030nm (see Figure 8). Obviously, the significant growth of ASE will limit the gain of our seed and this also is the reason why our slope efficiency is much lower than our expectation. To tackle this problem, the easiest way is to insert a bandpass filter between two stages to filter out the ASE generated in first stage[27]. So that such ASE won’t be further amplified in the second stage and thus suppress the growth of ASE. However, due to the limited components we have, we didn't have another bandpass filter to fulfill this job. As a result, instead of measuring the average power, we investigated the output spectrum after inserting the bandpass filter between two stages. Figure 19 shows that with the help of bandpass filter, the growth of ASE was suppressed, so we can believe that this method is work and could increases the seed saturation power and the slope efficiency of our YDFA.

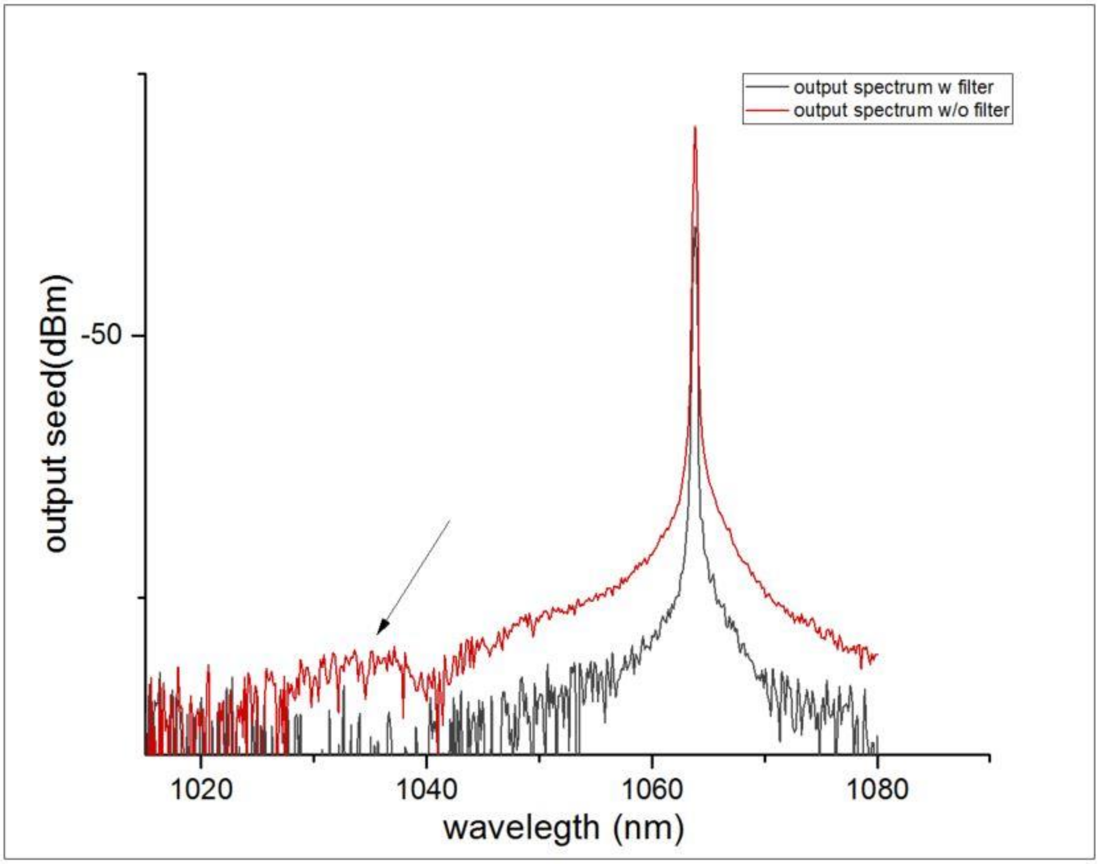

Figure 19: the output spectrum with and without inserting the bandpass filter between two stages

CHAPTER 5: CONCLUSION

In Summary, a numerical model and an experiment setup have been built. Based on rate equations, the numerical model is solved in steady state by using four order Runge-Kutta method and iteration. Through this model, we have a better understand on how the YDFA work, what limit the seed to be further amplified, and what the performance of YDFA will be under ideal condition. On the other hand, although we faced a lot of challenges when building the two stages YDFA setup, however, through tackling these challenges, we discovered many problems, that we never think about during modeling. For example, we didn't realize that angle cleaving is critical in YDFA until we start to build the experiment setup. Also, with the help of the setup, we investigated the spatial mode of seed and the spectrum growth, which can't be studied in our numerical model.

Overall, both the numerical model and the YDFA setup are useful and could help us to investigate YDFA theoretically and experimentally. However, there are still something we can do to improve them. First, many issues such as SPM, RBS, and Ramen effect, have not been considered in our model. Also, currently we only solve the rate equation in steady state so it isn't suitable for short pulse domain. Thus, next step is including the effect of SPM, RBS, as well as Ramen effect in our model, and extent the regime to short pulse domain. As to the experiment, currently our slope efficiency is much lower than what we expected and one possible solution is to insert a bandpass filter between two stages. Thus, we will buy another bandpass and use it to filter out the ASE generated in stage #1.

REFERENCES

[1] M. J. F. Digonnet, Ed., Rare Earth Doped Fiber Lasers and Amplifiers. New York: Marcel Dekker, 1993.

[2] R. Paschotta, J. Nilsson, A. C. Tropper, and D. C. Hanna, "ytterbium-doped fiber amplifiers," IEEE. J. Quantum Electron, vol. 33, pp. 1049-1059, July 1997.

[3] K. Kieu, B. G. Saar, G. R. Holtom, X. S. Xie, and F. W. Wise, "High-power picosecond fiber source for coherent Raman microscopy," Optics Letters, vol. 34, No. 13, pp. 2051-2053, July 2009.

[4] E. Snitzer, "Proposed fiber cavities for optical masers," Journal of Applied Physics, vol. 32, no. 1, pp. 36-39, 1961.

[5] R. J. Mears, L. Reekie, I. M. Jauncey, and D. N. Payne, "Low-noise erbium-doped fiber amplifier opearing at 1.54μm", Electron. Lett., vol. 23, pp. 1026-1028, 1987.

[6] E. Desurvire, C. R. Giles, J. R. Simpson, and J. L. Zyskind, "Efficient erbium-doped fiber amplifier at a 1.53-μm wavelength with a high output saturation power," Opt. Lett. 14, 1266-1268, 1989.

[7] Rui Song, Jing Hou, Shengping Chen, Weiqiang Yang, and Qisheng Lu, "157 W all-fiber high-power picosecond laser," Appl. Opt. 51, 2497-2500 (2012).

[8] J. M. Sousa, J. Nilsson, C. C. Renaud, J. A. Alvarez-Chavez, A. B. Grudinin, and J. D. Minelly, “Broad-Band Diode-Pumped Ytterbium-Doped Fiber Amplifier with 34-dBm Output Power,” IEEE Photonics, vol. 11, No.1, January 1999.

[9] Khanh Kieu, Brian G. Saar, Gary R. Holtom, X. Sunney Xie, and Frank W. Wise, "High-power picosecond fiber source for coherent Raman microscopy," Opt. Lett. 34, 2051-2053 (2009).

[10] Chen, Kangkang, Shaif-ul Alam, Dejiao Lin, Andrew Malinowski, and David J. Richardson. "100W fiberised linearly-polarized picosecond Ytterbium doped fiber MOPA." (2009).

[11] Wang, Yong, and Hong Po. "Dynamic characteristics of double-clad fiber amplifiers for high-power pulse amplification." Journal of lightwave technology 21, no. 10 (2003): 2262-2270.

[12] Liu, Hongjun, Cunxiao Gao, Jintao Tao, Wei Zhao, and Yishan Wang. "Compact tunable 10 W picosecond source based on Yb-doped fiber amplification of gain switch laser diode." In*Proc. World Academy Sci., Eng. Technol.*, pp. 379-382. 2010.

[13] Lee, Byoungho. "Review of the present status of optical fiber sensors." Optical fiber technology 9, no. 2 (2003): 57-79.

[14] J. T. Leonard, B. P. Yonkee, D. A. Cohen, S. Nakamura. “Nonpolar III-nitride vertical-cavity surface-emitting laser with a photoelectrochemically etched air-gap aperture.” Applied Physics Letters 108(3):031111, January 2016

[15] Joseph T. Verdeyen (1995). Laser Electronics (3rd Edition). Upper Saddle River, NJ: Pearson.

[16] Maryam Eilchi and Parviz Parvin (2016). Gain Saturation in Optical Fiber Laser Amplifiers, Fiber Laser, Dr. Mukul Paul (Ed.), InTech, DOI: 10.5772/62136.

[17] E. Snitzer, H. Po, F. Hakimi, R. Tumminelli, and B. C. McCollum, “Double-clad, offset core Nd fiber laser”, Optical Fiber Sensors, Vol. 2 of 1988 OSA Technical Digest Series (Optical Society of America, Washington, D. D., 1988), paper PD5.

[18] S.Chen, H. Chen, J. H, and Z. Liu, “100W all fiber picosecond MOPA laser”, Optics Express, vol. 17, no. 26, pp. 24008-24012, December 21, 2009.

[19] S. Wittek, R. Bustos Ramirez, J. Alvarado Zacarias, Z. Sanjabi Eznaveh, J. Bradford, G. Lopez Galmiche, D. Wang, W. Zhu, J. Antonio-Lopez, L. Shah, and R. Amezcua-Correa, "Mode-selective amplification in a large mode area Yb-doped fiber using a photonic lantern" Optics Letters 41(10), pp.2157-2160, May 15, 2016.

[20] R. Oron, A. Hardy, “Rayleigh backscattering and amplified spontaneous emission in high-power ytterbium-doped fiber amplifiers,” Opt. Soc. Am., vol. 16, no. 5, pp. 695-701, May 1999.

[21] Robert, L. (2014). Experiment and numerical study of a high-repetition rate Yb-fiber amplifier source. KTH Royal Institute of Technology. Sweden

[22] J. Marceron, H. Fevrier, J. Ramos, J. Auge, and P. Bousselet, “General theoretical approach describing the complete behavior of the erbium-doped fiber amplifier,” Fiber Laser Sources and Amplifiers II, vol. 1373, pp. 168-186, 1990.

[23] O. Svelto, Principles of Laser. Academic Press, 2007.

[24] Siamak Dawazdah Emami, Hairul Azhar Abdul Rashid, S. Z. M. Yasin, K. A. M. Shariff, M. I. Zulkifli, Zulfadzli Yusoff, Harith Ahmad, and Sulaiman Wadi Harun, "New Design of a Thulium–Aluminum-Doped Fiber Amplifier Based on Macro-Bending Approach," J. Lightwave Technol. 30, 3263-3272 (2012)

[25] C. Rangdy Giles and E. Desurvire “Modeling Erbum-Doped Fiber Amplifier,” journal of lightwave technology, vol. 9, no. 2, pp. 271-283, February 1991.

[26] E. Jaunart and P. Crahay, “Accurate EDFA modeling using a simple method,” Optical and Quantum Electron., vol. 27, pp. 881-886, 1995.

[27] Abrardi, L., Gusowski, M. A., & Feurer, T. (2014). High-fidelity all-fiber amplification of a gain-switched laser diode. Applied optics, 53(20), 4611-4615.